

University of New Mexico

UNM Digital Repository

Earth and Planetary Sciences ETDs

Electronic Theses and Dissertations

Summer 5-13-2024

Sub-Stage Climatic Shifts during MIS 11 Refined from Diatom Assemblage Reconstruction in the Valles Caldera, New Mexico

Savannah Cutler

Follow this and additional works at: https://digitalrepository.unm.edu/eps_etds



Part of the [Other Earth Sciences Commons](#), [Other Ecology and Evolutionary Biology Commons](#), [Paleobiology Commons](#), and the [Terrestrial and Aquatic Ecology Commons](#)

Recommended Citation

Cutler, Savannah. "Sub-Stage Climatic Shifts during MIS 11 Refined from Diatom Assemblage Reconstruction in the Valles Caldera, New Mexico." (2024). https://digitalrepository.unm.edu/eps_etds/413

This Thesis is brought to you for free and open access by the Electronic Theses and Dissertations at UNM Digital Repository. It has been accepted for inclusion in Earth and Planetary Sciences ETDs by an authorized administrator of UNM Digital Repository. For more information, please contact disc@unm.edu.

Savannah Cutler

Candidate

Earth and Planetary Science

Department

This thesis is approved, and it is acceptable in quality and form for publication:

Approved by the Thesis Committee:

Peter Fawcett , Chairperson

Rebecca Bixby

Tyler Mackey

**SUB-STAGE CLIMATIC STIFTS DURING MIS 11
REFINED FROM DIATOM ASSEMBLAGE
RECONSTRUCTION
IN THE VALLES CALDERA, NEW MEXICO**

by

SAVANNAH CUTLER

**BACHELORS OF ARTS
ENVIRONMENTAL STUDIES
VASSAR COLLEGE, 2020**

THESIS

Submitted in Partial Fulfillment of the
Requirements for the Degree of

**Master of Arts
Master of Earth and Planetary Sciences**

The University of New Mexico
Albuquerque, New Mexico

August, 2024

ACKNOWLEDGMENTS

I owe a tremendous thank you to Dr. Peter Fawcett, my advisor and dissertation chair, for encourage and believing in me throughout the past three years. Thank you to Dr. Becky Bixby, for without you and your diatom expertise my research would not possible. I cannot express how much each of your guidance and mentorship has impacted me, and I look forward to being able to apply what you've taught me as I continue my career. It truly has been a pleasure to collaborate with you.

I also thank my committee member, Dr. Tyler Mackey, for providing valuable feedback and suggestions that helped strengthen my interpretations.

To my best friend and Fiancé, Tristin, thank you for the many years of support and love you have given me. I wouldn't be where I am today without you.

And finally to my parents, your support has been the greatest gift of all. This thesis is dedicated to you, mom and dad.

**Sub-Stage Climatic Shifts during MIS 11 refined from Diatom Assemblage
Reconstruction in the Valles Caldera, New Mexico**

By

Savannah Cutler

B.A., Environmental Studies, Vassar College, 2020

M.S., Earth and Planetary Sciences, University of New Mexico, 2024

ABSTRACT

Diatom assemblage reconstruction from the Valles Caldera sediment core (VC-3) was utilized to infer climatic and aquatic changes during a 50-thousand-year [ka] period in the Mid-Pleistocene (435-385 ka). This 50 ka interval spans most of Marine Isotope Stage 11 (MIS 11) – one of the most prominent interglacials of the past 500 ka – and is widely considered an analog for the Holocene and future climate regimes. Nearly all records from MIS 11 are either marine or ice-core based, making VC-3 unique among lacustrine sediment records as it captures insolation variations and climatic changes during the mid-Pleistocene. Analysis of the diatom community assemblages shows rapid shifts between benthic (bottom-dwelling) and planktonic (free-floating) taxa, indicating the lake that occupied the Valle Grande within the Caldera experienced variable lake-levels. Autecology of dominant species (>10% relative abundance) allowed for the interpretation of water conditions and lake bathymetry during the mid-Pleistocene: taxa that thrive in cold, oligotrophic occur in abundance before Glacial Termination V; species indicative of higher nutrient-flux characterize transgressional and regressional events in the Lake's history; dominance of taxa that prefer shallow, eutrophic conditions occur coeval to mega-drought conditions; and low-density samples overlap with two ash-layer deposits (~397.2 and ~394.0 ka).

Table of Contents

1. INTRODUCTION	1
2. REGIONAL SETTING	3
2.1 <i>Study site</i>	3
2.2 <i>Modern Caldera climatology</i>	4
3. METHODS	5
3.1 <i>Sediment characteristics and chronology</i>	5
3.2 <i>Diatom processing</i>	5
3.3 <i>Analysis of diatom assemblages</i>	6
4. RESULTS	6
4.1 <i>Late-stage Core lithology</i>	6
4.2 <i>Diatom Stratigraphy</i>	8
4.3 <i>Non-metric multidimensional scaling (NMDS) of the diatom data</i>	12
5. DISCUSSION	14
5.1 <i>Diatom Autecology</i>	14
5.2 <i>Paleolimnological interpretation of diatom assemblages</i>	16
5.3 <i>Comparison to terrestrial data</i>	19
6. CONCLUSIONS	21
REFERENCES	23
SUPPLEMENTARY FIGURES	27

1. Introduction

Marine Isotope Stage 11 (MIS 11) (426 – 370 thousand years ago [ka]) was one of the most prominent mid-Pleistocene interglacials, lasting ~30 ka longer than all subsequent interglacials due to two obliquity-muted precessional cycles (Doxler & Farrell, 2000; Kleinen et al., 2014; Tzedakis et al., 2022). High concentrations of CO₂ and warm sea surface temperatures (SST) helped define MIS 11 as the first interglacial following the Mid-Brunhes Event (MBE) – a pivotal shift in the glacial-interglacial record where strong glacials give way to extended interglacials (Droxler & Farrell, 2000; Lang & Wolff, 2010; Kleinen et al., 2014; Tzedakis et al., 2022). Most records spanning this far back in time are either marine or ice-core-based, making the comparatively few MIS 11-aged terrestrial records ones of interest. In particular, long continuous lacustrine sequences are relatively rare registrars of terrestrial and aquatic feedbacks to past climate dynamics (Tzedakis et al., 2022).

Today, aridland freshwater ecosystems in the American Southwest are subjected to decreased flows and more pronounced effects of anthropogenic climate change. High turbidity from overland erosion and tributary contributions characterizes many riverine systems in New Mexico, particularly in the middle Rio Grande. Because of this, autochthonous primary production is compressed to littoral margins (“bathtub ring”) as light penetration is severely impacted in the pelagic zone of the water column. Furthermore, many aridland freshwater ecosystems in New Mexico are naturally nutrient-limited due to the phosphorus and silica-rich volcanic lithology. Understanding how aridland aquatic ecosystems responded in the past to climatic changes – such as mega-drought events during warmer climates – can inform our expectations for the future.

Paleoclimate studies conducted across the American West and Southwest have revealed dramatic glacial-interglacial climate changes driven by orbital forcings (Menking et al., 1997; Fawcett et al., 2011; Lachniet et al., 2014; Railsback et al., 2015a; Staley et al., 2021). Nearctic continuous lacustrine records (>100 Ka) from the continental U.S. are scarce and include: the Great Basin lake(s), California – Owens Lake (800 ka) (Menking et al., 1997 & Bradbury, 1997a/1997b), Mono Lake (200 ka) (Hodelka et al., 2020) and Lake Manix (~500 ka) (Reheis et al., 2012); Stoneman Lake (250 ka) Arizona (Staley et al., 2021); and the Valles Caldera basin (“Caldera”, ~560-320 ka) New Mexico (Fawcett et al., 2007). These

reconstructions are primarily based on terrestrial ecosystem proxies and have refined our understanding of how the arid Southwest responded to shifts in climate – such as extended drought conditions, glacial-interglacial transitions, and insolation forcing – during the Pleistocene.

However, comparatively less is known about how aridland freshwater ecosystems responded to climatic changes during Mid-Pleistocene interglacials in the American Southwest. Of the lakes mentioned above, only Owens Lake has been analyzed for fossil diatoms (Bradbury, 1997a; 1997b), which revealed strong associations between freshwater planktonic species during glacial periods and shallow-water saline species during drier, interglacial intervals. Two late-Pleistocene / Holocene paleoclimate studies from New Mexico (Markgraf et al., 1984; Menking et al., 2022) have applied diatom assemblage analysis, but are based on significantly younger deposits (age) than those reported upon in this study. The present study reconstructs the fossil diatom record from the Valles Caldera (35°N) New Mexico, the oldest of three young caldera-type volcanoes (Yellowstone, WY and Long Valley, CA) in the United States, to investigate changes the aquatic ecosystem underwent during a 50 ka interval spanning late-stage MIS 12 and MIS 11.

The catchments' response to climatic changes during the 50 ka interval in the Caldera is captured in the fossil diatom record due their sensitivity to water conditions and changes. Diatom microfossils are exceptional paleolimnological proxies owing to their generally well-preserved siliceous frustules and diverse distribution across different aquatic habitats, life history strategies and water-quality gradients (Smol, 2008; Rühland et al., 2015). Lake-level interpretations based on diatom assemblage reconstructions are well documented in both modern and paleo-limnology studies, and often rely on the ratio of planktonic (P, free floating) to benthic (B, littoral dwelling) species (Tapia et al. 2003; Ae et al., 2007; Stone, 2008; Rühland et al., 2015). Owing to their need to photosynthesize, diatoms are restricted to depths that receive enough sunlight. Littoral zones are near-shore areas where light penetrates all the way to the sediment-water interface and allows primary producers to grow (such as macrophytes and algae). Benthic species generally occupy this sediment-water interface in littoral zone environments, whereas planktonic species generally inhabit the upper region of a water column, or photic zone. Based on these habitat preferences, planktonic diatom species are often used to signify higher water levels and benthic diatom

species to signify lower water levels. However, stringent treatment of the P:B ratio without reference to a lake's bathymetry omits key physical characteristics that directly affect how water is held and distributed across a lake.

This research represents the first study of lacustrine fossil diatom assemblages in the Continental United States from the Mid-Pleistocene (435 – 385 [ka]), and helps to answer the following:

1) How did South Mountain Lake diatom assemblages in the Valles Caldera vary in response to climatic and environmental changes during the Mid-Pleistocene?

2) What can we infer about the hydrologic balance of South Mountain Lake? Can successional changes between diatom species be used to interpret bathymetry? and

3) Are there concurrent patterns between existing terrestrial proxy climatic data and South Mountain Lake diatom assemblages?

We hypothesize that the diatom assemblage reconstruction from the Valles Caldera will: (1) Allow for the interpretation of lake-level fluctuations: higher water levels during late-stage MIS 12 and lower water levels during megadrought conditions in MIS 11; (2) Show assemblage changes that mirror proposed lake bathymetry; and (3) Establish MIS 11 as a natural analog for future climate change in aridland aquatic ecosystems.

2. Regional Setting

2.1 Study site

The Valles Caldera National Preserve is situated among the Jemez Mountains in northern New Mexico, west of Los Alamos (Fig. 1). The caldera-forming eruption, and subsequent caldera collapse, of this ancient volcano occurred roughly 1.22 Ma and left a 22 km diameter depression in the landscape (Goff, 2009). Resurgence occurred almost instantaneously and uplifted Redondo Peak in the center of the caldera (Smith et al., 1968). A series of ring-fracture moat rhyolites erupted over the next million years, often temporarily blocking drainage from the Valle Grande and creating lakes in the Caldera's valleys after 0.8 Ma (Fawcett et al. 2007; Reneau et al. 2007; Goff, 2009). The Valle Grande (35° 52' N, 106° 28', 2553 m asl, catchment area 100 km²) is a section of the Caldera that did not experience uplift and remained at a lower elevation in relation to the surrounding resurgent domes and Caldera moat (Goff, 2009). A lake formed after the emplacement of South Mountain rhyolite

near the southwest end of the Valle Grande at 552 +/- 3 ka (based on ^{40}Ar - ^{39}Ar dating of tephra), which blocked ancestral East Fork Jemez River drainage from the catchment. The lake – hereafter referred to as South Mountain Lake – occupied the Valle Grande for ~200 ka before complete desiccation (Fawcett et al., 2007; Goff, 2009).

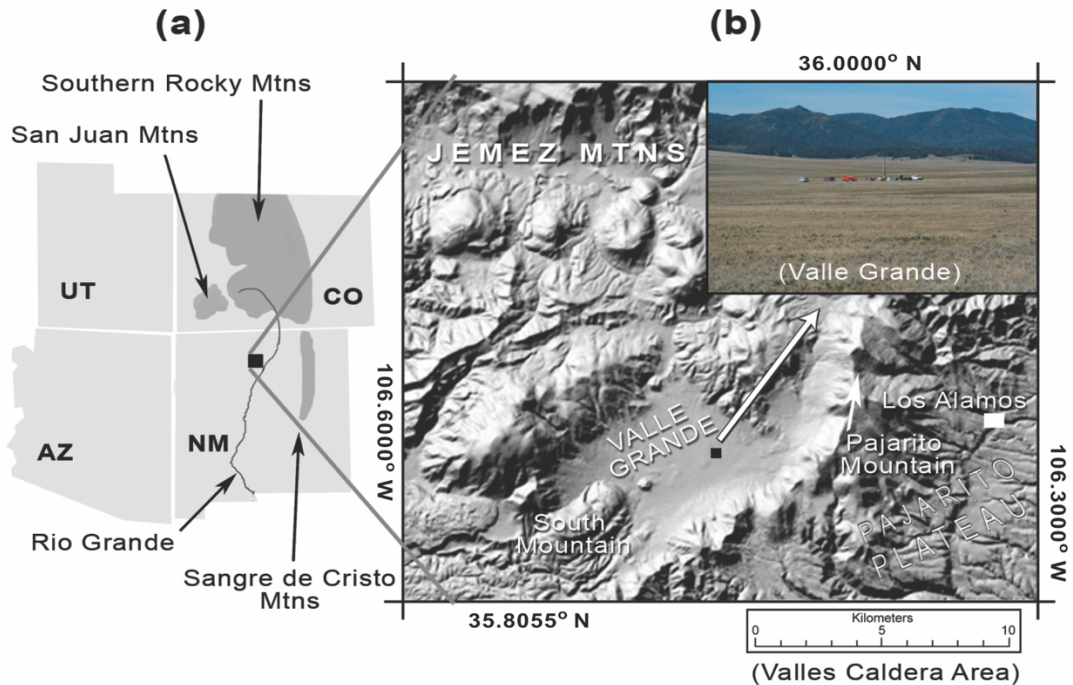


Figure 1 (A and B). Regional map of the Valles Caldera location and topographic features in the immediate vicinity modified from Fawcett et al. (2011). The Valle Grande (35°52'N, 106°28'W, 2553 m asl) is marked above and is the drill site for VC-3.

2.2 Modern Caldera climatology

The Valle Grande's modern climate is monitored from a USCRN co-op weather station (NM Los Alamos 13 W) at the Valles Caldera National Preserve headquarters. Mean annual temperature (MAT) of this site is 4.8°C with summer (JJA) temperatures averaging 14.0°C and winter (DJF) temperatures averaging -4.5°C. Annual precipitation usually occurs during the summer and winter (~670 mm total) with drier spring and fall seasons. Precipitation source differs between summer and winter: summer precipitation totals average 260 mm (~40% of the annual total) due to convective monsoons, whereas winter (DJF) totals average 180 mm due to frontal precipitation during the 3-month season (~26% of the annual total) (Fawcett et al., 2011). Valles Caldera National Preserve sits at 8,000 ft at its lowest topographic point, ranging up to 11,254 ft at its highest point – Redondo peak. Elevation strongly influences vegetation communities within the Caldera: Riparian wetlands and

Montane grasslands give way to Montane forests in a steppe fashion as elevations increase, creating an inverted treeline (Coop, 2007).

3. Methods

3.1 *Sediment characteristics and chronology*

Sediment core VC-3 was recovered during a 2004 collaborative drilling project in the Valle Grande and consists of 82 m of lacustrine silts and clays with interspersed layers of gravels and muds (Fawcett et al., 2007) (Fig. 1). Prior to splitting, the whole round-core sections were logged and analyzed at 1-cm intervals for magnetic susceptibility, gamma ray densitometry, electrical resistivity, and P-wave velocity (Fawcett et al., 2007). After the core was split, the u-channel was stored in the Quaternary Laboratory at the University of New Mexico – separate from the rest of the core which is stored at the Limnological Research Center National Lacustrine Core Facility & Repository (LacCore) at the University of Minnesota. VC-3 chronology and lithology, MAT, fossil pollen, total organic carbon (TOC), C/N, Si/Ti, $\delta^{13}\text{C}$, and δD analyses were reported in previous studies (Fawcett et al. 2007; Fawcett et al. 2011; Cisneros-Dozal et al., 2014; Contreras et al., 2016).

Dating of the core was achieved through ^{40}Ar - ^{39}Ar dating of a glassy tephra (74.8 m) and a well-sorted pumiceous gravel (76.0 m), generating an age of 552 +/- 3 ka which constrains the onset of lacustrine sedimentation to MIS 14 in the middle Pleistocene (Fawcett et al., 2011). Further paleomagnetic data (progressive alternating field demagnetization) correlated two short-lived negative magnetic field events (at 17.25 m and 52.3 m) to globally recognized events at 11 α (400 ka.) and 14 α (536 ka) (Lund et al., 2006). Two abrupt increases in bulk properties (TOC, Carbon/Nitrogen ratio, Si/Ti ratio) were correlated with Glacial Terminations VI (533 ka) and V (426 ka) (Lisiecki & Raymo, 2005; Fawcett et al., 2011). While the entire core spans the middle Pleistocene from MIS 14 (552 +/- 3 ka) to MIS 10 (~360 ka), this study focuses on a ~50 ka interval between 435 ka and 385 ka (Fawcett et al., 2011).

3.2 *Diatom processing*

Following the Stoermer et al. (1995) method for processing sediments, each 1-cc sample was treated with 30% hydrogen peroxide and nitric acid to oxidize organic material. Samples were then serially rinsed with distilled water and decanted 8 times to remove

oxidation byproducts, and subsequently evaporated onto 18 mm round coverslips using a combination of circular evaporation trays developed by Battarbee (1973) and hot plate(s), before being mounted to microscope slides using Zrax for light microscopy. Approximately 500 diatom valves were enumerated and identified to lowest taxonomic level (usually species) along transects using a Leica 4500 compound microscope with brightfield and differential interference contrast optics at 1100x magnification. Individual diatom valves along each transect were enumerated by size relative to whole valves (i.e. 25%, 50%, 75%, 100%), and transformed to whole-valve units in the total count (Connelly et al., 2008). In seven samples with extremely low diatom densities (>100 valves present) occurring between ~ 400 ka – 393 ka, 10 transects were examined (180 mm total) before counts were terminated. Species identification was completed using taxonomic literature (Bahls, 2021; Camburn and Charles, 2000; Krammer and Lange-Bertalot, 1991; Krammer 1989) and the Diatoms of North America (DoNA) Taxon Identification Guide (Spaulding et al., 2010). Counts are reported as percentages.

3.3 Analysis of diatom assemblages

A threshold value of >10% total assemblage was applied to classify dominant species; the 22 species that met this threshold were analyzed using the following statistical and graphical methods in R (citation):

(1) Cluster analysis (CONISS) and the resultant Bray-Curtis dissimilarity matrix of diatom assemblage changes using the R rioja package (v1.0-6) (Juggins, 2020). South Mountain Lake diatom zones (SML-D11; SML=South Mountain Lake; D11=Diatom assemblages from late-stage MIS 12 and MIS 11) were interpolated from the broken-stick model's significant clusters (Bennet, 1996).

(2) Non-metric Multidimensional Scaling (NMDS) to synthesize how constituent species and assemblage composition changes from one community to the next in the core, using the R vegan package.

4. Results

4.1 Late-stage Core lithology

South Mountain Lake lithology from late-stage glacial MIS 12 and interglacial MIS 11 has distinct facies (~435-388 ka), each representing different climate regimes experienced

in the Caldera. Below is a brief outline of visual sedimentation changes the core captured during late-stage MIS 12 and stage MIS 11 (Fig. 2):

Finely laminated, light-colored sediment indicative of a deep, established lake system characterized late-stage MIS 12 (3020-2740 cm depth; ~435-425 ka). The light-colored sediment abruptly give way to darker, more organic-rich material at 2782 cm – directly correlating to Glacial Termination V (426 ka). Organic-rich sediment continued to accumulate in fine laminations until 2490 cm (~419.5 ka), where it becomes more thickly bedded. Loss of laminations is inferred to signal lower water level in the Valle Grande aquatic system. The sudden onset of a gleyed horizon event at 2430 cm – where low oxygen conditions reduce ferrous minerals to produce grey-colored sediments – is interpreted to represent a transgressional period, where water-levels dropped dramatically in South Mountain Lake. A 1-meter deep mudcrack begins at ~2400 cm (~417.0 ka) and extends back until ~2566 cm and is attributed to megadrought conditions noted in Fawcett et al. (2011). Gleyed conditions continue with intermittent bedding until 2330 cm (~415.0), culminating in a 1-cm thick layer of fine, light-colored material. Accumulation of organic-rich laminations occurs directly after the cessation of the gleyed conditions and continue uninterrupted until two 1-cm thick layers of volcanic ash – occurring at 1636 cm (~397.2 ka) and at 1553 cm (~394.0 ka)– constrain a segment of organic-poor sediment. Laminated, organic-rich sediment (1553 – 1350 cm depth) resumes immediately after the 1553 cm ash layer and defines the remaining core lithology of the 50 ka interval.

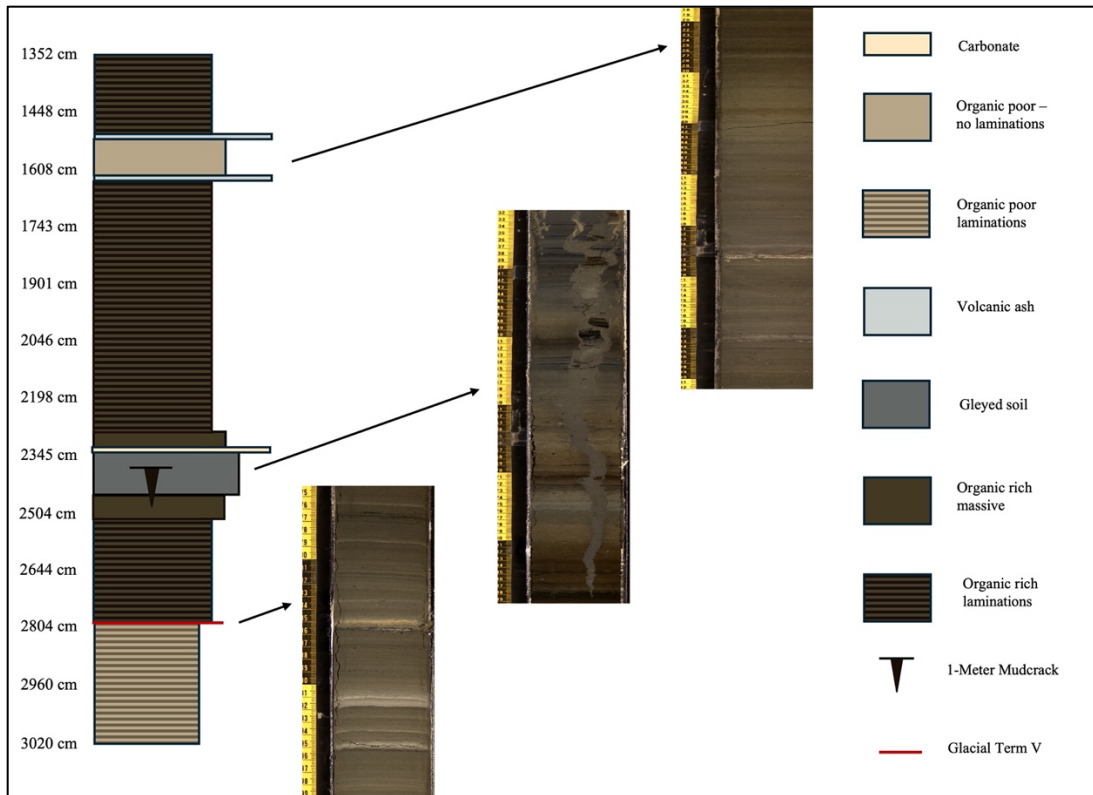


Figure 2. Late-stage MIS 12 and MIS 11 VC-3 core lithology from South Mountain Lake. Glacial Termination V is represented by a red line. The 1-meter Mudcrack is represented by a black triangle. Lithologic facies: Cream = carbonate; Light brown = organic poor-no laminations; Light brown-striped = organic poor laminations; Light Grey = volcanic ash; Dark grey = Gleyed soil; Dark brown = organic rich massive; Dark brown-striped = organic rich laminations.

4.2 Diatom Stratigraphy

Diatom stratigraphy was constrained to late-stage MIS 12 and stage MIS 11-aged core sections (~435-388 ka) from the South Mountain Lake sequence, with 51 samples analyzed (Fig. 3). For discussion purposes, staurosiroids are grouped together (i.e., *Staurosira construens*, *Staurosira leptostauron* var. *dubia*, *Staurosirella martyi*, *Staurosirella pinnata*) due to similar morphology and ecological preferences. Below are brief narratives of the dominant species in each South Mountain Lake diatom (SML-D11) zone and their respective abundances based on the Bray-Curtis dissimilarity and CONISS cluster analysis (Fig. 3; Table 1).

Zone SML-D11 A. Staurosiroids-*Lindavia* sp.01-*Aulacoseira alpigena* (2720-3020 cm, 8 samples, ~425.0-434.7 ka). This zone encapsulates the end of glacial MIS 12, ending at the glacial-interGlacial Termination V transition (426 ka). The Bray-Curtis dissimilarity and subsequent cluster analysis indicates this zone is the most different from the other zones, which is to be expected as this is the late glacial stage of MIS 12 while other zones occur

within interglacial MIS 11. Moderately high abundances of *Lindavia* sp.01 (20%-30%) and *Aulacoseira alpigena* (~10-20%) characterize the planktonic community, with similar moderate to high abundances seen in the littoral-dwelling staurosiroids (20%-40%). *Pinnularia borealis* var. *linearis* (17%), *Cocconeis neodiminuta* (8%), and *Planolithidium jour.* (9%) each experience their respective maxima at various points throughout this zone. Slight increases in *Aulacoseira pusilla* (~10%) and *Lindavia intermedia* (2%) proceed the glacial-interglacial transition that distinguishes this glacial zone from those zones in MIS 11.

Zone SML-D11 B. *Lindavia intermedia*- *Aulacoseira pusilla*- *Aulacoseira alpigena*- *Discostella* sp. (2635-2720 cm, 4 samples, ~423.0-425.0 ka). Complete decline of all abundant benthic species and *Lindavia* sp.01 is at antiphase with dramatic increases in *L. intermedia* (53%) and *A. pusilla* (34%) that each peak at their highest abundances. *Aulacoseira alpigena* also sees a major decline as *L. intermedia* and *A. pusilla* reach their maxima. This zone also features most prominent spike in abundance of *A. alpigena* (40%), coinciding with a moderate rise in *Discostella* sp. (12%). Both *A. alpigena* and *L. intermedia* decrease in abundance until fully disappearing from the zone by 423 ka.

Zone SML-D11 C. *Lindavia radiosa*-*Stephanodiscus niagarae* (2430-2635 cm, 6 samples, ~418.0-423.0 ka). *Stephanodiscus niagarae* surges to a secondary maximum (65%) as it fully replaces *A. alpigena*, *L. intermedia* and *Discostella* sp. before plummeting to complete disappearance at (421.61 ka). Accompanying this is a sharp peak in *L. radiosa* (66%) and relatively low abundances of *L. intermedia* (16%) and *Discostella* sp. (9%). Immediately after, *S. niagarae* reappears to reach its primary maximum (73%) and persists in high abundances until the end of the zone.

Zone SML-D11 D. *Lindavia intermedia*-*Ellerbeckia arenaria* forma *teres*-*Epithemia musculus*-*Cymbellonitzschia diluviana* (2260-2430 cm, 5 samples, ~413.5-418.0 ka) begins with a rapid decline and immediate cessation of *S. niagarae* that persists through the remainder of the zone. In its absence, moderate spikes in *Ellerbeckia arenaria* forma *teres* (15%) and *Lindavia intermedia* (31%) occupy the zone before tapering off by ~414 ka. Benthics diversify as *Campylodiscus clypeus* (10%), *Cocconeis placentula* (7%), *Cymbellonitzschia diluviana* (20%), *Gogorevia exilis* (13%), *Epithemia musculus* (16%), and staurosiroids (~20%) each undergoing moderate peaks in abundances.

Zone SML-D11 E. *Stephanodiscus niagarae*-*Discostella* sp.-*Lindavia* sp. (2050-2260cm, 5 samples, ~408.5-413.5 ka). *Stephanodiscus niagarae* dominates this zone, with its highest abundance (80%) before fluctuating between 36% - 59%. Concurrent with the fluctuations in *S. niagarae* are moderate rises in *Lindavia* sp.01 (27%), *Discostella* sp. (18%), and *Lindavia* sp.02 (9%).

Zone SML-D11 F. *Discostella* sp.-*Stephanodiscus niagarae*-Staurosiroids-*Aulacoseira ambigua* (1690-2050 cm, 12 samples, ~399.0-408.5 ka). This zone is defined by variable *Discostella* sp. (0%-49%) and *S. niagarae* (0%-42%) abundances that peak and trough at different intervals in the zone. Staurosiroids have moderate to high abundance(s) – around (~30%) with various increases up to (~60%). *Aulacoseira ambigua* (41%) arises suddenly and sustains its' maximum at 406.4 ka before dissipating completely; *Aulacoseira alpigena* (24%) displays a similar trend at 408.1 ka.

Zone SML-D11 G. Staurosiroids-*Stephanodiscus niagarae*-*Cocconeis placentula*-*Lindavia intermedia* (1580-1690 cm, 3 samples, ~395.0-399.0 ka). This zone is defined largely for its samples having extremely low densities (5-60 valves per 180 mm). The spikes in abundances for staurosiroids, *S. niagarae*, *C. placentula*, *L. intermedia*, *E. arenaria* forma *teres*, and *A. alpigena* in this zone should all be scrutinized closely in relation to each samples' total count (Table 2; Appendix).

Zone SML-D11 H. Staurosiroids-*Stephanodiscus niagarae*-*Lindavia bodanica* (1352-1580 cm, 9 samples, ~388.3-395.0 ka). Low diatom densities continue persist until 393 ka, . Staurosiroids maintain variable high abundances throughout the zone (~40%-60%) alongside moderate *S. niagarae* (0%-30%) oscillations. *Lindavia bodanica* (24%) flashes in at 394.6 ka for its one and only appearance, and quickly disappears after. The planktonic community diversifies as *A. ambigua* (16%), *A. alpigena* (13%), *Discostella* sp. (12%), *E. arenaria* forma *teres* (18%), *Lindavia* sp.01 (9%), and *Lindavia* sp.02 (16%) each undergo moderate increases in abundance.

SML-D11 H	1630-1690	~397.0-399.0	Staurosiroids- <i>Cocconeis placentula-Lindavia intermedia</i>
SML-D11 I	1580-1630	~395.0-397.0	Staurosiroids- <i>Stephanodiscus niagarae</i>
SML-D11 J	1352-1580	~388.3-395.0	Staurosiroids- <i>Stephanodiscus niagarae-Lindavia bodanica</i>

4.3 Non-metric multidimensional scaling (NMDS) of the diatom data

The NMDS yielded a non-metric fit (R^2) of 0.979 and stress of 0.144 after 21 iterations (Fig. 4). The diatom NMDS1 axis separates benthic species (*C. clypeus*, *E. musculus*, *G. exilis*) and planktonic species (*L. intermedia*, *A. pusilla*, *E. arenaria* forma *teres*) towards the positive end, while planktonic species, such as *S. niagarae*, *A. ambigua*, are grouped towards the negative end of this axis. The diatom NMDS2 axis further separates benthic species (e.g., *C. clypeus*, *E. musculus*, *G. exilis*) from all other species, placing them close to the negative extreme of this axis; *S. niagarae* separates from *A. ambigua* (more negative and more positive, respectively); *L. bodanica* is separate from all other species as it is plotted on the positive extreme of this axis; *Cymbellonitzschia diluviana* and *L. radiosa* are grouped towards the negative end; and remaining species (e.g., *C. placentula*, *C. neodiminuta*, *P. lanceolata*, *P. joursacense*, *S. construens*, *S. pinnata*, *Lindavia sp.01*, and *Discostella sp.*) are centralized around zero. Overlain are polygons corresponding to the eight zones (SML-D11 A-H), with zones C/E and F/H plotting close together while zones A, B, D and G are separated either by the NMDS1 and/or NMDS2 axis. Axes scores (NMDS1/NMDS2/NMDS3) were extracted and are plotted against time in Fig. 5.

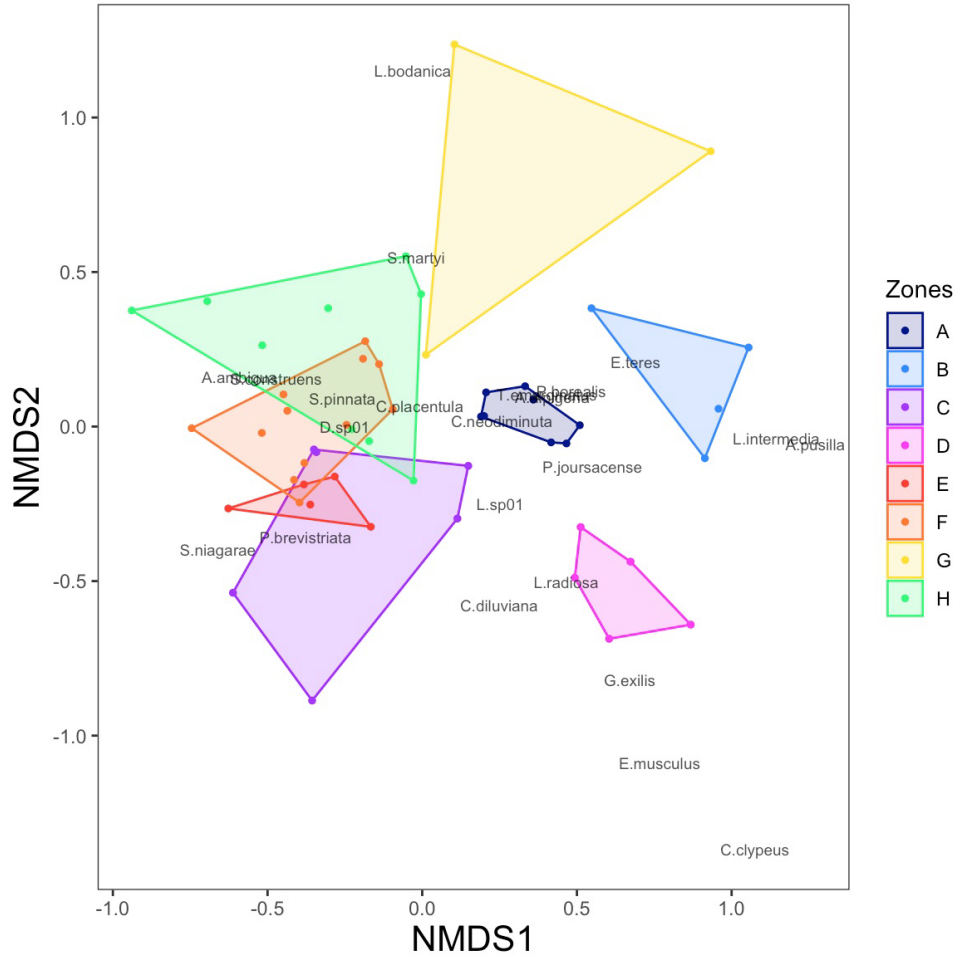


Figure 4. Non-metric multidimensional scaling (NMDS) ordination applied to dominant diatom species, plotting the NMDS1 and NMDS2 axes. Points and polygons are color-coordinated to their corresponding SML-D11 zones: Zone A = Navy; Zone B = Blue; Zone C = Purple; Zone D = Pink; Zone E = Red; Zone F = Orange; Zone G = Yellow; and Zone H = Green. Species names are plotted in relation to their NMDS1 / NMDS2 scores.

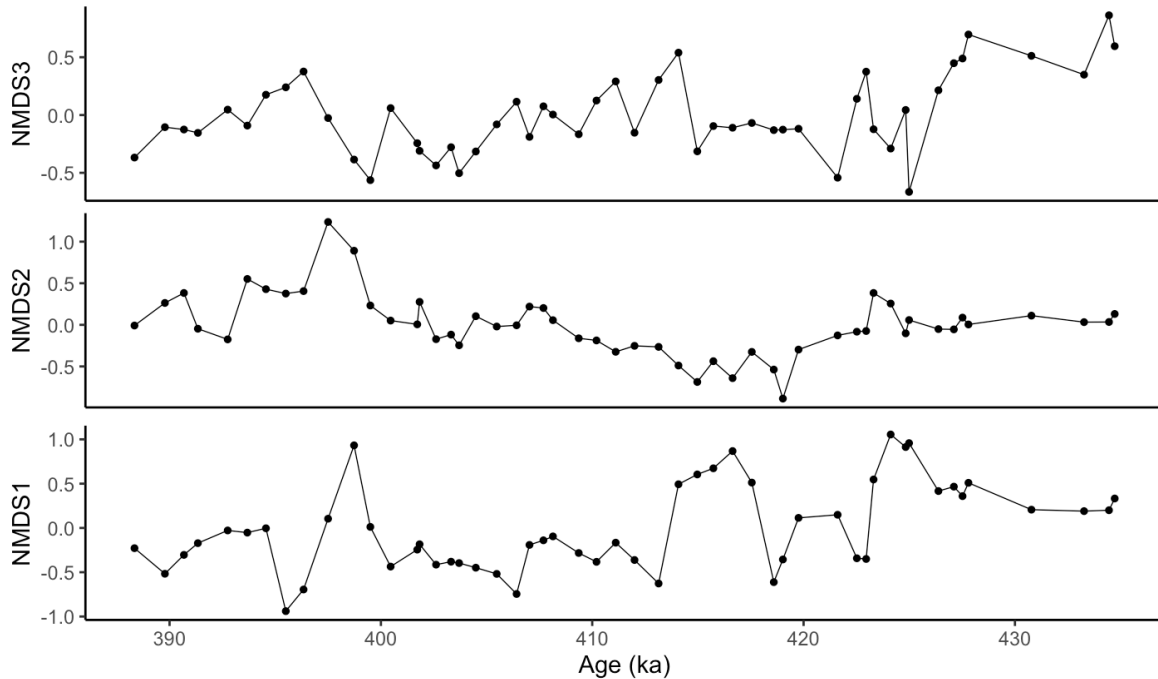


Figure 5. NMDS axes scores plotted against time (ka). NMDS3 is the topmost plot; NMDS2 is the second plot; and NMDS1 is the bottommost plot. Highlights changes in NMDS axis scores over time.

5. Discussion

5.1 Diatom Autecology

While the SML-D11 record includes roughly ~140 different taxa, autecology information of the dominant species (>10% total assemblage) allowed us to interpret changes the aquatic regime underwent utilizing shifts in the SML-D11 assemblages. Planktonic species dominate most of the SML-D11 zones, and identification down to species allowed for further interpretations of water conditions and water-column structure. *Aulacoseira* is typically a heavily silicified, chain-forming tycho planktonic genus that relies on strong water-column mixing (Anderson et al., 1996; Fritz et al., 2019; Wang et al., 2022; Dias et al., 2023). Two *Aulacoseira* species (*A. alpigena* and *A. pusilla*) occur in high abundances during Glacial Termination V: *Aulacoseira alpigena* thrives in cold, circumneutral waters with a tolerance to low nutrient conditions (Anderson et al., 1995; Fritz et al., 2019; Bahls, 2021; Dias et al., 2023); and *Aulacoseira pusilla* is noted in oligotrophic, alpine lakes – with its abundances controlled mainly by water transparency (i.e. more light penetrating down into water column = blooms of *A. pusilla*) (Pedraza Garzon and Saros, 2022). *Lindavia intermedia* has been reported in cold, alkaline waters with low nutrients and conductivity

(Bahls, 2021). *Lindavia radios*a has been observed to thrive in shallow, transparent alpine water bodies with moderate access to nutrients (Malik et al., 2016; Bahls, 2021; Yu et al., 2023). *Stephanodiscus niagarae* is a large planktonic species indicative of higher nutrient conditions (particularly nitrogen) in cool, alpine aquatic systems (Bahls, 2021; Streib et al., 2021; Avendaño et al., 2023). The staurosiroids flourish in littoral zones and shallow water environments and are often considered pioneer species whose high rate of reproduction allows for the rapid colonization of expanding or contracting aquatic environments (Finkelstein and Gajewski, 2008; Bahls, 2021; Díaz et al., 2023).

Along with these taxa are subdominant species that although are not numerous, document changes in the hydrologic balance of South Mountain Lake over time. In particular, species which only occur during SML-D11 zone D offer a more nuanced understanding of the hydrologic balance of South Mountain Lake under extended drought conditions. *Epithemia musculus* utilizes a symbiotic relationship with nitrogen-fixing cyanobacteria to convert nitrogen gas into ammonia they can use during periods of low-N, signifying more oligotrophic conditions (You et al., 2009; Spaulding, 2010). *Campylodiscus chlypeus* is commonly found in inland, brackish water environments with moderate to high concentrations of carbonate and sulfate (Fritz et al., 1993; Poulíčková & Jhan, 2007; Menking et al., 2023). *Gogorevia exilis* is a small benthic species typically found in weakly alkaline lakes with low to moderate conductivity (Taylor et al., 2014; Kulikovskiy et al., 2020). Similarly, *Cymbellonitzschia diluviana* is found in alkaline waters and is considered a ruderal species that can withstand high habit disturbance (Jewson & Lowry, 1993). Occurrence of these benthic species coincide with abundances of *Ellerbeckia arenaria* forma *teres*, which has a circumpolar to circumboreal distribution in oligotrophic, slightly alkaline standing waters with high transparency and moderate calcium concentrations (Evans, 1964; Rawlence, 1992; Houk et al., 2017).

In addition to these lacustrine species, *Cocconeis placentula* and *Cocconeis neominuta* are found in oxygen-rich, slightly alkaline waters along littoral zones in lakes (Bradbury 1997; Toporowska et al., 2008; Moser & Kimball, 2009; Menking et al., 2022). The remaining species – *A. ambigua*, and *L. bodanica* – are both reported in modern studies to be alkaliphilous and inhabiting cool, oligotrophic conditions ranging from the hypolimnion up to surface waters (Saros et al., 2012; Malik et al., 2016; Bahls, 2021).

5.2 Paleolimnological interpretation of diatom assemblages

Sedimentation in the Caldera following desiccation of South Mountain Lake in-filled the lake basin so that any shoreline deposits have since been buried under thick layers of silt, gravel, and siliciclastic sediments. Reconstruction of South Mountain lake's bathymetry is therefore inferred from both the sedimentological record of VC-3 core and successional pattern(s) of species before and immediately after the megadrought conditions. We envision the bathymetry of South Mountain Lake (Fig. 6) as having steep sides and extremely shallow extended margins so that a two-part sequence occurs during regressive events. Initial decreases in water-level cut off the littoral zones but support a planktonic community in the remaining water column; the secondary decrease further lowers the water-column so that benthic species are able to colonize the exposed profundal lake bottom.

An established, relatively deep lake system with an active littoral zone and low nutrient flux characterizes the oldest SML-D11 zone A (~425-434 ka), which encapsulates the glacial maxima of MIS 12 at termination V (Fig. 6(A)). The zone features moderately high abundances of *Lindavia* sp.01 and Staurosiroids, modest abundances of *A. alpigena*, and low abundances of *C. placentula*, *C. neodiminuta*, and *P. joursacense* (Fig. 2). The assemblage of benthic and planktonic communities during late-stage MIS 12 implies the Valle Grande catchment was inundated enough to develop a productive littoral zone, as well as support a deeper pelagic profile. Finely laminated, lightly colored sediments deposited throughout this zone help to corroborate this interpretation. The Bray-Curtis dissimilarity also recognized the community structure to be very different from the successive SML-D11 zones.

Abrupt transitions in both the sedimentological and diatom data occurs at 426 ka, where previous communities that characterized SML-D11 A decline sharply and light-colored sediments give way to darker, more organic rich material at 2898 cm depth. This is directly correlated to Glacial Termination V. We see a dramatic community shift from *Lindavia* sp.01 and Staurosiroids dominating to *L. intermedia*, *A. pusilla*, and *A. alpigena* each undergoing their highest peaks in abundance between ~425-423 ka. This is interpreted to signify restructuring of the water column, where the stability that characterized the late-stage MIS 12 lake is succeeded by moderate levels of disturbance and turbulence as water

begins to recede in the catchment (Fig. 6(B)). A decline in littoral environments is suggested to coincide with this disturbance as benthic abundances dramatically decrease.

This regressive event, where we envision the water level dropping below a shallow-shelf zone and an overall increase in available nutrients, defines the community assemblage shift during ~423-418 ka. We see this reflected in laminations still present in the organic-rich sediment and in the sudden onset of extremely high abundances of *S. niagarae* and *L. radiosa*. As the water-level in South Mountain Lake continued to drop (Fig. 6(C)), water transparency allowed for sunlight to penetrate down to the bottom of the lake and supported low abundances of benthic-dwelling Staurosiroids. The extreme contemporaneous decline in *S. niagarae* and sharp, ephemeral spike in *L. radiosa* at 421.6 ka indicates a fleeting change in the hydrologic balance as effective precipitation decreased and allowed for the rapid succession of *L. radiosa* to the detriment of *S. niagarae*.

A prominent change in the SML-D11 record begins at ~418 ka, consisting of a community shift that sees a complete disappearance of *S. niagarae* from this zone prior to the diversification of benthic species. Sedimentary laminations are replaced by more massive layers that abruptly transition to a gleyed horizon event at 2430 cm. Gleysol sediment persists throughout the rest of this zone, encapsulating a 1-meter-deep mud-crack that begins at 2430 cm depth and extends back until 2467 cm. Previous interpretations concluded the Valle Grande completely desiccated during this time. However, the presence of both benthic and planktonic species that tolerate high levels of disturbance, high concentrations of carbonates and nitrogen-limited conditions offers a more nuanced understanding of the hydrologic balance in the lake basin during extreme drought conditions. Shallow pools are conjectured to have remained in the Valle Grande despite megadrought conditions (Fig. 6(D)), with moderate abundances of benthic species (*C. clypeus*, *C. diluviana*, *E. musculus*, *G. exilis* and *S. ruckii*) and planktonic species (*E. arenaria* forma *teres*, *L. intermedia*) occurring during this zone ~418-413.5 ka. The diatom NMDS2 axis expresses the prominent assemblage change as values abruptly drop to negative between ~418 and 413 ka (Fig. 5). Additionally, intermittent laminations within the gleysol sediments suggest the retention of deeper-water pockets that allowed for undisturbed deposition.

Cessation of gleyed conditions directly correlate to the Bray-Curtis dissimilarity break that occurs at ~413.5 ka between SML-D11 D & E (2334 cm depth). Immediate

reprisal of assemblage members present before the extensive drought conditions in SML-D11 D indicates water-levels began to rise in the catchment, further corroborated by the accumulation of organic-rich laminations. *S. niagarae* peaks at its maximum abundances at 413.4 ka and is interpreted to have been caused by a moderate in-flux of nutrients. The NMDS1 / NMDS2 plot overlaps SML-D11 zones C and E (Fig. 4), suggesting that the conditions leading up to and immediately following the gleyed event shared similar hydrologic characteristics. Return to a deeper water profile in the Valle Grande was gradual and eventually allowed for the reestablishment of shallow littoral environments along the lake's margins (Fig. 6(E)). Staurosiroids regain moderate abundances at ~409 ka as *S. niagarae* begins a variable decline that is accompanied by conspicuous increases in *Discostella* sp., each of which continue until ~399 ka. Two short-lived spikes in *A. ambigua* (406.4 ka) and *A. alpigena* (408.1 ka) are interpreted to represent periods of lake turnover in an otherwise moderately stable water-column during SML-D11 zone E.

At 400 ka, a sequence of diatom-poor samples begins and lasts until ~393 ka, implying a major transition in the Valle Grande's environmental conditions. Two volcanic ash layers (1636 cm, ~397.3 ka; 1553 cm, ~394.5 ka) constrain a section of organic-poor sediment, which might offer a plausible explanation for the low diatom densities. Additionally, increased sedimentation is hypothesized to occur contemporaneously with the deposition of these two ash layers. Nearly all diatom valves present in these samples were broken to some degree, with only small heavily silicified Staurosiroids remaining intact. There was a noticeable increase in siliciclastic sediments and volcanic glass abundance in the samples under light microscopy analysis, which corroborates the ash fall event (Fig. 6(F)). Abundances quickly return to previous levels after 393 ka as Staurosiroids and *S. niagarae* reappear, concurrent with short-lived spikes in *L. bodanica*, *E. arenaria* forma *teres*, *Discostella* sp., *A. ambigua*, and *A. alpigena* throughout the rest of this zone.

Fossil diatom records from the continental U.S. are rare, with only one other lake record – Owens Lake, California (Bradbury, J., 1997) – spanning the late Pleistocene, making comparisons challenging. In addition, only a few global lacustrine records from the mid-to-late Pleistocene utilize diatom assemblage analysis: Lake Titicaca, Peru (Fritz et al., 2012); Lake Baikal, Russia (Edlund et al., 1998); Lake Ohrid, Macedonia (Edlund et al., 2019); East African Lakes in the East African Rift Zone (Stone, 2011); and Lake Biwa,

Japan (Kuwaie et al., 2002). Each of these records occupied vastly different ecological and geological distributions, complicating comparisons to them as they experienced different climate regimes and orbital forcing signals.

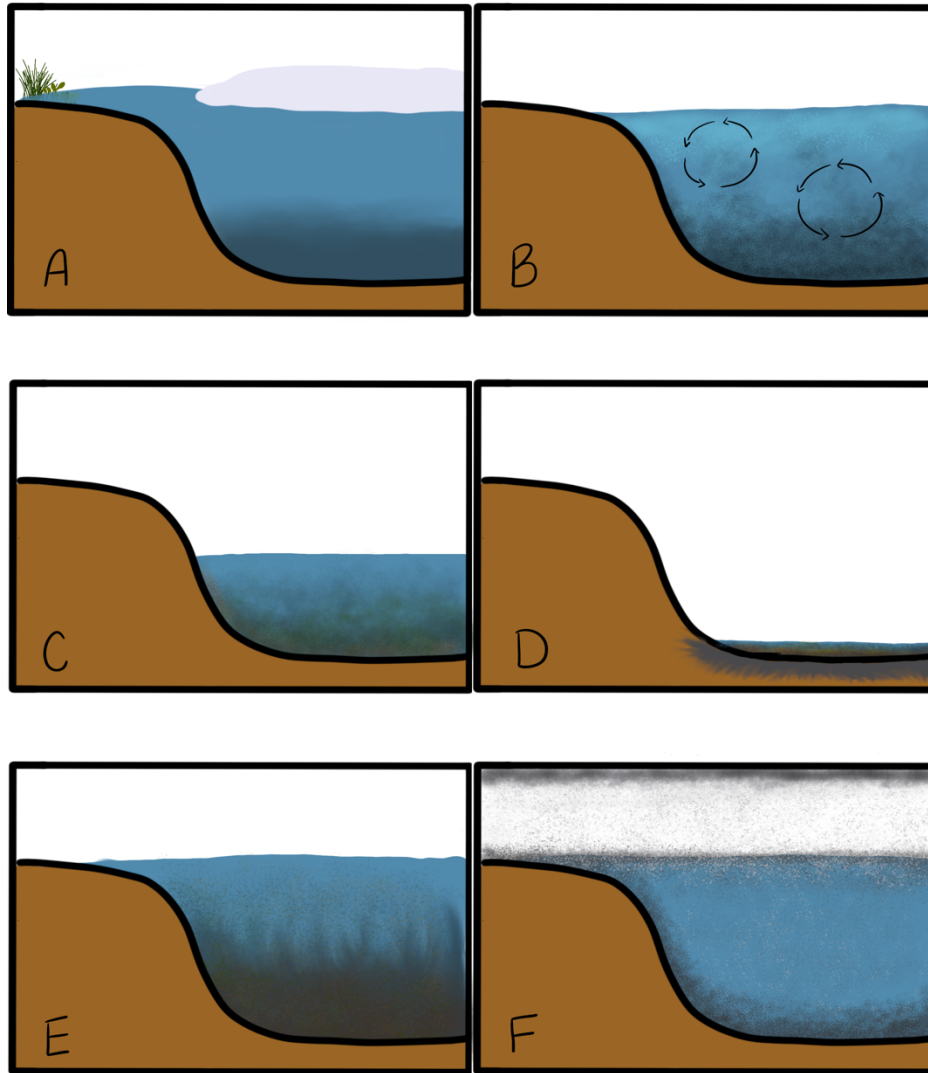


Fig. 6. Proposed South Mountain Lake bathymetry throughout different climatic changes experienced between 435-385 ka. A) Late-Stage glacial MIS 12; B) Glacial Termination V; C) Regression as water-levels drop; D) Mega-drought / Gleyed Conditions; E) Transgression as water-levels rise; & F) Volcanic ash deposition / increased sedimentation.

5.3 Comparison to terrestrial data

Terrestrial data reported in Fawcett et al. (2011) from the Valles Caldera show high rates of change throughout late-stage MIS 12 and MIS 11. Proxies such as MBTd/CBT (Glycerol Dialkyl Glycerol Tetraether (GDGT) membrane lipids from soil bacteria) giving

MAT, Si:Ti ratio, Ca counts, and TOC% revealed five distinct substages, three warm and two cool substages, within MIS 11 (Supplemental Fig. 1). Comparison of these terrestrial proxies against the changes in lake-level inferred from diatom assemblages during the ~50 ka interval between (435-385 ka) distinguished concurrent patterns (Fig. 7).

An established, oligotrophic lake with a productive littoral zone characterized late-stage 12 as MAT hovered around (-2°C) before dropping to a negative excursion (-6°C) at 426 ka (MIS 12 glacial maximum). Low-nutrient conditions in the lake are concurrent with low TOC% values, Si:Ti ratio and Ca counts. The P:B ratio (Fig. 7) during SML-D11 zone A – within the context of South Mountain’s bathymetry (Fig. 6) – is interpreted to align with a completely inundated catchment with shallow margins. As temperatures began to rebound at Glacial Termination V, a dramatic spike in the P:B ratio occurred that represents a decline in benthics coeval with an increase in planktonics. The Si:Ti ratio captures this increase in diatom productivity, albeit with a lag of a few hundred years. Additionally, increases in TOC% and Si:Ti coincide with the interpretation of a reduced catchment area as water-levels begin to drop and available nutrients rise as temperatures warm. And although increasing, MAT fluctuates before reaching a peak of ~7°C at 408 ka.

Drought conditions experienced in the Valle Grande, previously inferred from the extreme jump in scanning XRF Calcium concentrations (i.e. counts) and dramatic TOC% decline, is contemporaneous with near-desiccation of the catchment. However, presence of diatoms species that tolerate high levels of disturbance suggest retention of shallow water-bodies. The P:B ratio indicates near complete dominance of benthic species during SML-D11 zone D as P:B values hover near 0%. Return of deeper water in the catchment is reflected in higher P:B ratios, Si:Ti ratios and TOC% values immediately after drought conditions terminate. Elevated TOC%, with a relatively low P:B ratio throughout SML-D11 zone E, supports the interpretation of the re-establishment of shallow margins as South Mountain Lake re-fills to full capacity.

The zone of low diatom densities is coeval with a significant decrease in insolation, decrease in overall TOC%, and low Si:Ti ratios. Aquatic ecosystem production declined in this interval due to increased sedimentation (and likely turbidity) within the Valle Grande catchment.

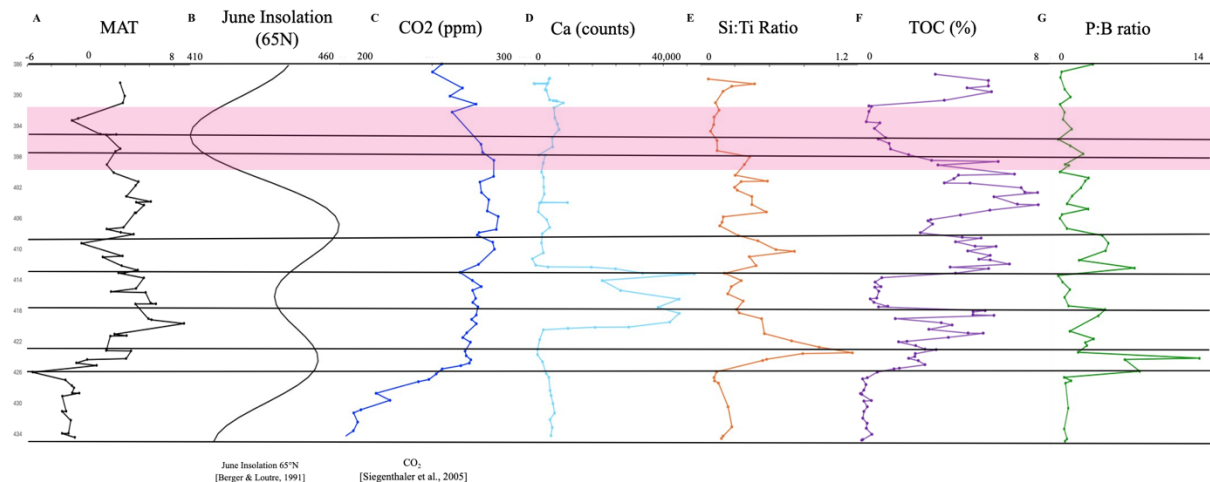


Figure 7. Reconstructed temperature, bulk geochemical proxy data and P/B ratio from VC-3 record. (A) Mean annual temperature [MAT (°C)] based on branched glycerol dialkyl glycerol tetraether distribution (Weijers et al., 2007). (B) June insolation at 65°N (Berger & Loutre, 1991). (C) Measured atmospheric CO₂ concentrations (Siegenthaler et al., 2005). (D) Calcium XRF counts (E) Si:Ti ratio from core scanning X-ray fluorescence (XRF). (F) Total organic carbon concentration. (G) P/B data from this study

6. Conclusions

The fossil diatom record of SML-D11 successfully reconstructs lake-level history in the Valle Grande catchment during late-stage MIS 12 and MIS 11. The reconstruction is in agreement with terrestrial data that shows strong associations between the shifts in diatom assemblage and MAT, TOC% and Ca count fluctuations. Succession of species occurs in discrete, rapid events which allowed for the interpretation of the onset, duration and strength of lake-level fluctuations. Lake bathymetry was also inferred from the successional pattern(s) of species before and immediately after the megadrought conditions: initial decreases in water level cut off the shallow littoral margins and increase concentrations of planktic species; subsequent decline after water-level falls below the shallow-self zone follows traditional P:B ratio scenarios, where benthic abundances increase and planktonic abundances decrease as the water-column shrinks. The converse effect is noted to occur as lake-levels begin to increase.

Within the diatom assemblage structures themselves, dominant species abundances allowed for further interpretations of nutrient flux, water column structure, and overall water conditions. Staurosiroids are indicative of both productive littoral zones and extremely low water-levels; *Aulacoseira* species abundance indicates water-column restructuring and increased turbidity due to lake turnover; *Lindavia* species indicate oligotrophic periods with a relatively stable water-column under different aquatic temperatures in SML-D11;

Stephanodiscus niagarae is one of the only dominant planktonic species to represent increased nutrient-flux and more mesotrophic conditions, as well as warmer water temperatures; and species occurring only during the extensive drought conditions – *Campylodiscus clypeus*, *Cymbellonitzschia diluviana*, *Epithemia musculus*, *Gogorevia exilis*, and *Surirella ruckii* – represent high levels of disturbance within the Valle Grande catchment as high concentrations of carbonates and N-limited conditions cause complete collapse of previously dominant community structures. This new diatom record from the Valles Caldera substantiates a variable aquatic ecosystem during late-stage MIS 12 and MIS 11 and adds key details to the story of how the paleo-lake changed in response to local, regional and orbital climate forcings.

References

- Anderson, N.J., *et al.* (1996) 'Climate-lake interactions recorded in varved sediments from a Swedish boreal forest lake', *Global Change Biology*, 2, pp. 399–403.
- Avendaño, D *et al.* (2023) 'Response of diatom assemblages to orbital- and millennial-scale climatic variability since the penultimate glacial maximum in the northern limit of the Neotropics', *Journal of Quaternary Science*, 38, pp. 750-766. <https://doi.org/10.1002/jqs.3507>
- Battarbee, R.W., (1973) 'A new method for estimation of absolute microfossil numbers, with reference especially to diatoms', *Limnology and Oceanography*, 18(4), pp. 647-653.
- Bahls, L. (2021) 'Diatoms of Montana and Western North America: Catalog and Atlas of Species in the Montana Diatom Collection', *The Academy of Natural Sciences of Philadelphia, Special Publication*, (1)24, pp. 1-508.
- Berger, A., & Loutre, M. F. (1991) 'Insolation values for the climate of the last 10 million years', *Quaternary Science Reviews*, 10(4), pp. 297–317. [https://doi.org/10.1016/0277-3791\(91\)90033-Q](https://doi.org/10.1016/0277-3791(91)90033-Q)
- Bradbury, J.P. (1997)a 'A diatom-based paleohydrology record of climate change for the past 800 k.y. from Owens Lake, California', *Geological society of America Special Paper*, 317, p. 99-112.
- Bradbury, J.P. (1997)b 'A Diatom record of climate and hydrology for the past 200 KA from Owens Lake, California with comparison to other great basin records', *Quaternary Science Reviews*, 16, p. 203-219.
- Camburn, K.E. & Charles, D.F. (2000) 'Diatoms of Low-Alkalinity Lakes in the Northeastern United States', *Academy of Natural Sciences of Philadelphia, Special Publication* 18, 152.
- Connelly, S., *et al.* (2008) 'Changes in Stream Primary Producer Communities Resulting from Large-Scale Catastrophic Amphibian Declines: Can Small-Scale Experiments Predict Effects of Tadpole Loss?', *Ecosystems*, 11, pp. 1262–1276. <https://doi.org/10.1007/s10021-008-9191-7>
- Coop, J.D. and Givnish, T.J. (2007) 'Gradient analysis of reversed treelines and grasslands of the Valles Caldera, New Mexico' *Journal of Vegetation Science*, 18, pp. 43-54. <https://doi.org/10.1111/j.1654-1103.2007.tb02514.x>
- Díaz, C., *et al.* (2023) 'Freshwater diatom evidence for Southern Westerly Wind evolution since ~18 ka in northwestern Patagonia', *Quaternary Science Reviews*, 316(108231). <https://doi.org/10.1016/J.QUASCIREV.2023.108231>
- Edlund, M. B. (1998) 'Paleoecological evidence of climate change and historical patterns of planktonic diatom diversity inferred from the Lake Baikal (Russia) sediment record', *University of Michigan*.

- Edlund, M. B. (2013) 'Diatoms as indicators of environmental change in ancient Lake Ohrid during the last glacial–interglacial cycle (ca. 140 ka)', *Phycologia*, 52(4), pp. 379–380. doi: 10.2216/13-BR2.1.
- Evans, G.H., (1964) 'Two fossil diatoms from the lake deposits of the English Lake District', *New Phytologist*, 63(3), pp. 413–417.
- Fawcett, P.J., *et al.* (2007) 'Two Middle Pleistocene Glacial-Interglacial Cycles from the Valle Grande, Jemez Mountains, northern New Mexico', *New Mexico Geological Society Guidebook, 58th Field Conference, Geology of the Jemez Mountains Region II*, p. 409-417.
- Fawcett, P.J., *et al.* (2011) 'Extended megadroughts in the southwestern United States during Pleistocene interglacials', *Nature (London)*, 470(7335), pp. 518-521.
- Finkelstein, S.A., *et al.* (2008) 'Responses of fragilarioid-dominated diatom assemblages in a small arctic lake to Holocene climatic changes, Russell island, nunavut, Canada', *Journal of Paleolimnology*, 40, pp. 1079–1095.
- Fritz, S.C., *et al.* (2004) 'Patterns of early lake evolution in boreal landscapes: a comparison of stratigraphic inferences with a modern chronosequence in Glacier Bay, Alaska', *Holocene*, 14(6), pp. 828–840.
- Fritz, S. C., *et al.* (2012) 'Evolution of the Lake Titicaca basin and its diatom flora over the last~ 370,000 years', *Palaeogeography, Palaeoclimatology, Palaeoecology*, 317, pp. 93-103.
- Fritz, S.C. & Anderson, N.J., (2013) 'The relative influences of climate and catchment processes on Holocene lake development in glaciated regions', *Journal of Paleolimnology*, 49, pp. 349–362.
- Fritz, S.C., *et al.* (2019) 'Long-term and regional perspectives on recent change in lacustrine diatom communities in the tropical Andes', *Journal of Paleolimnology*, 61, pp. 251–262.
- Heinsalu, A. *et al.* (2008) 'Water level changes in a large shallow lake as reflected by the plankton:periphyton-ratio of sedimentary diatoms', *Hydrobiologia*, 599, pp. 23–30. <https://doi.org/10.1007/s10750-007-9206-y>
- Hodelka, B. N., *et al.* (2020) 'Paleoproduction and environmental change at Mono Lake (eastern Sierra Nevada) during the Pleistocene-Holocene transition', *Palaeogeography, Palaeoclimatology, Palaeoecology*, 543(109565). <https://doi.org/10.1016/J.PALAEO.2019.109565>
- Houk, V., *et al.* (2017) 'Atlas of freshwater centric diatoms with a brief key and descriptions. Second emended edition of Part I and II', *Melosiraceae, Liparogyraceae, Paraliaceae and Aulacoseiraceae. Fottea* 17(Supplement): 1-616.
- Jewson, D.H., *et al.* (1993) '*Cymbellonitzschia diluviana* Hustedt (Bacillariophyceae): Habitat and auxosporulation', *Hydrobiologia*, 269, pp. 87–96. <https://doi.org/10.1007/BF00028008>

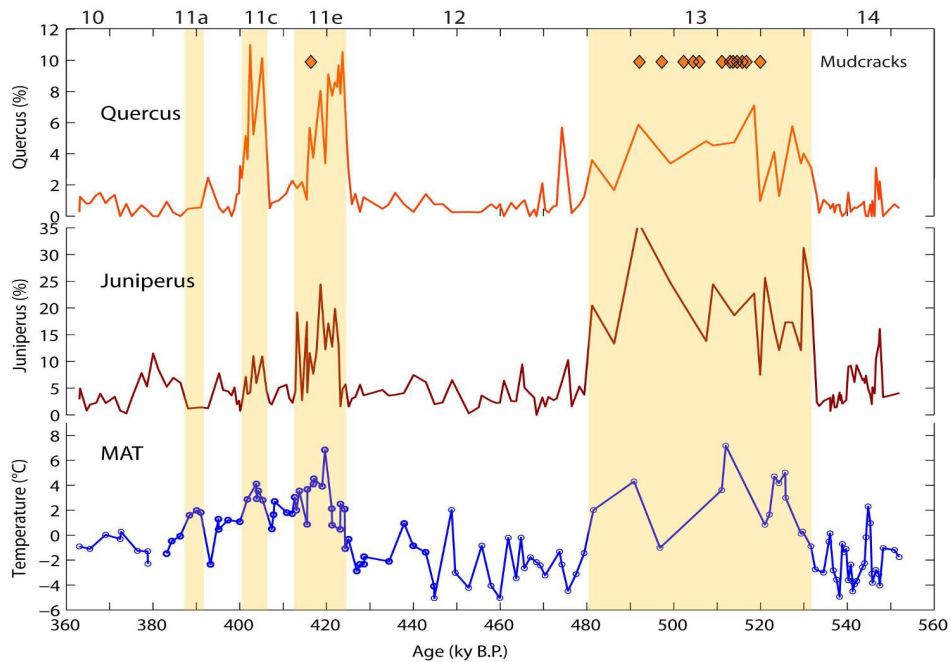
- Juggins, S., (2020) 'Rioja: Analysis of Quaternary Science Data, R Package Version (0.9- 26)', <https://cran.r-project.org/package=rioja>
- Krammer, Kurt. (1989) 'FUNCTIONAL VALVE MORPHOLOGY IN SOME SURIRELLA SPECIES (BACILLARIOPHYCEAE) AND A COMPARISON WITH THE NAVICULACEAE1', *Journal of Phycology*, 25, pp. 159-167. 10.1111/j.0022-3646.1989.00159.x.
- Krammer, K. & Lange-Bertalot, H.(1991) 'Bacillariophyceae 4. Teil Achnanthaceae Kritische Ergänzungen zu Navicula (Lineolatae) und Gomphonema', *Gesamtliter at Urverzeichnis*, 14.
- Kulikovskiy, M., *et al.* (2020), 'Gogorevia, a New Monoraphid Diatom Genus for *Achnanthes exigua* and Allied Taxa (Achnanthidiaceae) Described on the Basis of an Integrated Molecular and Morphological Approach', *Journal of Phycology*, 56, pp.1601-1613. <https://doi.org/10.1111/jpy.13064>
- Kuwae, M., *et al.* (2002) 'A diatom record for the past 400 ka from Lake Biwa in Japan correlates with global paleoclimatic trends', *Palaeogeography, Palaeoclimatology, Palaeoecology*, 183(3-4), pp. 261-274.
- Lachniet, M., *et al.* (2014) 'Orbital control of western North America atmospheric circulation and climate over two glacial cycles', *Nature Communications*, 5(3805). <https://doi.org/10.1038/ncomms4805>
- Malik, H.I., *et al.* (2017), 'Nutrient limitation status of Arctic lakes affects the responses of *Cyclotella sensu lato* diatom species to light: implications for distribution patterns', *Polar Biology*, 40, pp. 2445–2456. <https://doi.org/10.1007/s00300-017-2156-6>
- Markgraf, V., *et al.* (1984) 'San Agustin Plains, New Mexico: Age and Paleoenvironmental Potential Reassessed', *Quaternary Research*, 22, pp. 336-343. 10.1016/0033-5894(84)90027-9.
- Menking, K.M., *et al.* (1997). Climatic/Hydrologic Oscillations since 155,000 yr B.P. at Owens Lake, California, Reflected in Abundance and Stable Isotope Composition of Sediment Carbonate. *Quaternary Research*;48(1):58-68. doi:10.1006/qres.1997.1898
- Menking, K.M., *et al.* (2022) 'Diatom evidence for a groundwater divide that limited the extent of Lake Estancia, New Mexico, USA, highstands during the Last Glacial Maximum', *GSA Bulletin*, 135. 10.1130/B36283.1
- Railsback, L.B., *et al.* (2015)a. A record of wet glacial stages and dry interglacial stages over the last 560kyr from a standing massive stalagmite in Carlsbad Cavern, New Mexico, USA: *Palaeogeography, Palaeoclimatology, Palaeoecology*, 438, pp. 256–266. <https://doi.org/10.1016/j.palaeo.2015.08.010>.
- Rawlence, D.J. (1992) 'Paleophycology of Long Lake, Saint John County, New Brunswick, Canada, based on diatom distribution in sediments', *Canadian Journal of Botany*, 70(2), pp. 229–239
- Reheis, M. C., *et al.* (2012) 'A half-million-year record of paleoclimate from the Lake Manix Core, Mojave Desert, California', *Palaeogeography, Palaeoclimatology, Palaeoecology*, 365–366, pp. 11–37. <https://doi.org/10.1016/J.PALAEO.2012.09.002>

- Rühland, K.M., *et al.* (2015) 'Lake diatom responses to warming: reviewing the evidence', *Journal of Paleolimnology*, 54, pp. 1–35. <https://doi.org/10.1007/s10933-015-9837-3>
- Spaulding, S.A., *et al.* (2010) Diatoms of the United States <http://westerndiatoms.colorado.edu>
- Staley, S.E., *et al.* (2021) 'Early Pleistocene–to–present paleoclimate archive for the American Southwest from Stoneman Lake, Arizona, USA', *GSA Bulletin*, 134(3-4), pp. 791–814. doi: <https://doi.org/10.1130/B36038.1>
- Stone, J. R. (2005) 'A high-resolution record of Holocene drought variability and the diatom stratigraphy of foy lake, montana', Retrieved from <https://libproxy.unm.edu/login?url=https://www.proquest.com/dissertations-theses/high-resolution-record-holocene-drought/docview/305460014/se-2>
- Stone, J. R., *et al.* (2011) 'Late Pleistocene paleohydrography and diatom paleoecology of the central basin of Lake Malawi, Africa', *Palaeogeography, Palaeoclimatology, Palaeoecology*, 303(1–4), pp. 51–70. <https://doi.org/10.1016/J.PALAEO.2010.01.012>
- Taylor, J., *et al.* (2014) 'Analysis of the type of *Achnanthes exigua* GRUNOW (Bacillariophyta) with the description of a new Antarctic diatom species', *Journal of the Czech Phycological Society*, 14, pp. 43–51. 10.5507/fot.2014.003.
- Tapia, P. M., *et al.* (2003) 'A Late Quaternary diatom record of tropical climatic history from Lake Titicaca (Peru and Bolivia)', *Palaeogeography, Palaeoclimatology, Palaeoecology*, 194(1–3), pp. 139–164. [https://doi.org/10.1016/S0031-0182\(03\)00275-X](https://doi.org/10.1016/S0031-0182(03)00275-X)
- Tzedakis, P. C., *et al.* (2022) 'Marine Isotope Stage 11c: An unusual interglacial', *Quaternary Science Reviews*, 284(107493). <https://doi.org/10.1016/J.QUASCIREV.2022.107493>
- Yu, S., *et al.* (2023) 'Spatial distribution of surface-sediment diatom assemblages from 45 Tibetan Plateau lakes and the development of a salinity transfer function', *Ecological Indicators*, 155(110952).
- Wang, J., *et al.* (2022). Seasonal variations of diatoms in a low-latitude mountain lake: a case study from Douhu lake-Southeast China. *Diatom Research*, 37, pp. 165–178.

Supplementary Figures

Supplementary Table 1. Total count values for the 7 samples in the low-density zone.

Section	SML-D11 Zones	Depth (cm)	Age (kyr)	Total Count
9H-1 55-56	H	1523	393.68	63
9H-1 83-84	H	1551	394.56	274
9H-1 113-114	H	1581	395.5	37
9H-1 140-141	H	1608	396.34	32
9H-2 27-28	G	1645	397.5	7.5
9H-2 66.5-67.5	G	1684	398.73	5.75
9H-2 91-92	G	1709	399.5	132.5



Supplementary Fig. 1. *Quercus* and *Juniperus* pollen reconstruction from Fawcett et al. (2011). Both pollen assemblages spike during the warmest sub-stage periods (11a, c and e), trending closely with MAT, while dropping off during the two cool sub-stages in between. The Orange diamonds represent mud cracks observed throughout MIS 13 and 11.